Journal of Modern Optics
Publication details, including instructions for authors and subscription information:
http://www.informaworld.com/smpp/title~content=t713191304

Low dispersion surface plasmon-polaritons on deep silver gratings

Z. Chen [a]; I. R. Hooper [a]; J. R. Sambles [a]
[a] Thin Film Photonics Group, School of Physics, University of Exeter. EX4 4QL, Exeter. UK

To link to this article: DOI: 10.1080/09500340600578179
URL: http://dx.doi.org/10.1080/09500340600578179

Journal of Modern Optics
Vol. 53, No. 11, 20 July 2006, 1569–1576

Low dispersion surface plasmon-polaritons on deep silver gratings

Z. CHEN, I. R. HOOPER and J. R. SAMBLES*

Thin Film Photonics Group, School of Physics,
University of Exeter, Exeter, EX4 4QL, UK

(*Received 9 December 2005; in final form 13 January 2006*)

Surface plasmon modes supported by short-pitch silver gratings with different depths have been characterized by studying the reflectivity as a function of the angle of incidence and the incident wavelength (400–850 nm). Highly non-dispersive 'flat' surface plasmon-polariton bands were found corresponding to localized, within the grooves, radiative resonant modes. Experimental reflectivities were compared with model calculations and to help understand the character of each of the modes, the optical magnetic field distributions at the resonant frequencies were explored.

1. Introduction

In 1902 Wood reported the observation of a series of anomalies, which were only found for transverse magnetic (TM) polarization, in the reflectivity spectra from ruled metallic gratings [1]. Fano [2] was the first to provide a theoretical model of the resonance anomalies observed, developing a theory of surface plasmon-polaritons (SPPs) at a metal dielectric interface. A SPP is a fundamental electromagnetic (EM) excitation on a metal–dielectric interface, which is confined to the surface. On a flat metal surface, a SPP mode cannot be directly excited by incident radiation in the dielectric because the wave vector of the SPP is always beyond that of a grazing incidence photon-polariton of the same frequency. On a metallic grating, however, the SPP dispersion curve splits into bands, just as the electronic states in a periodic potential form into bands, making direct coupling between the SPP and radiation modes possible. In effect, in-plane momentum may be provided by the grating periodicity to match the SPP excitation condition. In the regime of shallow gratings, which have a small ratio between their pitch and depth (distance from peak to trough), the excitation of SPPs on metal gratings can be very well described by perturbation theory [3] and much experimental evidence for these electromagnetic resonances has been reported. It is well known that for shallow metallic grating structures the SPP can only be excited in a small corner of the dispersion curve in

*Corresponding author. Email: J.R.Sambles@exeter.ac.uk

Journal of Modern Optics
ISSN 0950–0340 print/ISSN 1362–3044 online © 2006 Taylor & Francis
http://www.tandf.co.uk/journals
DOI: 10.1080/09500340600578179

the zero-order (non-diffracting for all angles of incidence) region. The reason for this is that even with the added momentum available to the incident radiation due to scattering from the grating, the momentum of the SPP on such a structure is still close to the grazing photon momentum and it is thus excited just beyond the diffraction edge. However, for high aspect ratio metallic monogratings the SPP dispersion curve may be so severely modified that resonant absorption of light due to SPP excitation may occur well within the zero-order region of the spectrum. It has been shown that such structures can display very strong optical features. Sobnack *et al.* [4] modelled the scattering of EM waves from zero-order silver gratings at a fixed wavelength and noted that as the grating depth is increased a set of reflection minima occur due to the excitation of SPP modes localized in the deep grooves. Also, Porto *et al.* [5] evaluated the optical band structures for lamellar transmission gratings with a pitch of 3.5 μm and a depth of 4 μm and showed flat-banded resonances in the infrared region of the spectrum. In other previous studies, Tan *et al.* [6] and Hooper and Sambles [7] calculated the dispersion of SPPs for short-pitch deep metal gratings and found that very flat SPP bands are formed in the zero-order region of the spectrum. These flat-banded resonances are very different to the SPPs excited on shallow gratings, and have been explained as being due to hybrid waveguide-SPP resonances.

For shallow gratings significant band-gaps form in the SPP dispersion curve when the grating profile contains a $2k_g$ component (k_g being the grating vector) [8, 9]. Scattering from this $2k_g$ component allows the forward and backward propagating SPPs to couple together to form two standing wave states with different energies. These are thus excited at different frequencies with a forbidden region (band-gap) between, with the size of the band-gap being largely determined by the amplitude of the $2k_g$ component in the grating profile. Of course, as well as scattering from the $2k_g$ component, two scattering events from the fundamental k_g component of the grating will also produce a band-gap, though this process is much weaker.

If the grating has a sufficiently large $2k_g$ component, or, in the case of a sinusoidal grating, has sufficient amplitude, the band-gaps formed may be substantial. This means that the lower energy branches at the band-gaps reduce in frequency sufficiently such that even on a zero-order grating some of these may be coupled to at all angles of incidence. A more detailed description of the formation of these flat bands can be found elsewhere [7].

Note in addition that in very deep channels in good conductors standing-wave waveguide resonances may be excited. These may be regarded as open-ended organ pipe modes [10]. Thus for very deep gratings the lower branch modes at or near the band-gaps become essentially waveguide resonances. It is therefore clear that in the visible region of the spectrum the modes have a hybrid nature which is both SPP-like and waveguide-mode-like simultaneously.

Despite the conceptual and practical interest of these resonances and well-documented theoretical predictions, until now almost no experimental evidence of these hybrid electromagnetic resonances has been reported for visible optical frequencies.

In the present study, we utilize photoresist gratings as replica templates to fabricate silver gratings with a pitch of 258 nm and depths of 124 nm and 166 nm.

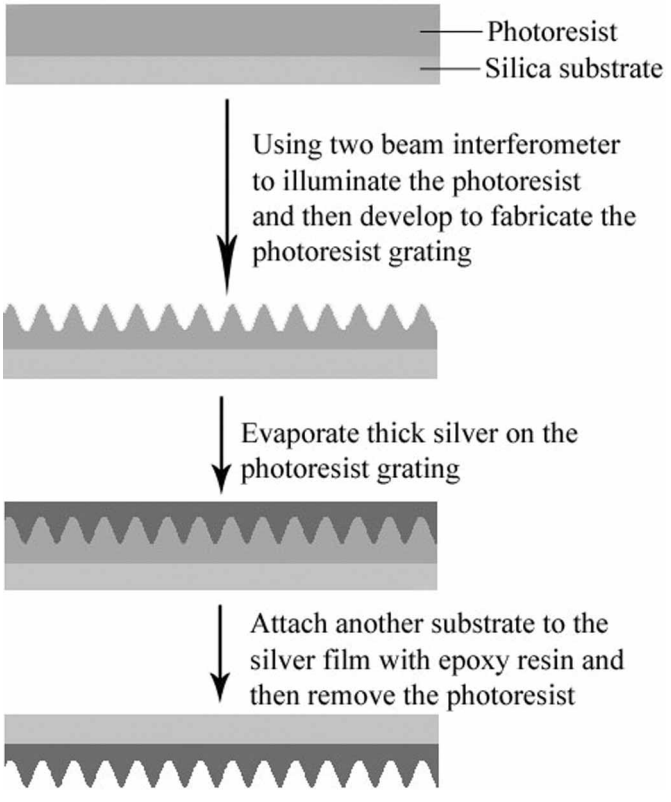

Figure 1. Schematic of the fabrication of the silver gratings. First a photoresist-coated silica substrate is exposed to two expanded collimated interfering beams. Development removes exposed regions, producing the expected grating in the photoresist. Thick silver is evaporated on to these gratings. Then another substrate is attached to the silver film with epoxy resin. After removing the photoresist using acetone, the silver grating is prepared with the same pitch and depth as the photoresist grating, but reversed profile.

Through comparing the reflectivities as both functions of the angle of incidence and incident wavelength ($400\,\text{nm} < \lambda_0 < 850\,\text{nm}$) for these silver gratings with different depth, we show that the SPP bands are compressed, shifting to lower frequencies and becoming flatter as the grating depth increases. In the zero-order region of the spectrum these form, as predicted, flat SPP bands for very deep gratings.

The scheme for fabricating the deep silver gratings is shown in figure 1. First a Shipley S1400-17 photoresist coated silica substrate is exposed to two expanded collimated interfering beams of UV laser light ($\lambda = 325\,\text{nm}$), recording the interference fringes as a solubility profile in the photoresist. Development removes the more soluble (exposed) regions, producing an amplitude grating in the photoresist. Depositing silver on these deep gratings results in a very rough silver-air interface grating which gives strong optical scatter. To avoid this we use instead the photoresist gratings as replica templates by first evaporating very thick silver onto them, then attaching a substrate to the surface of the silver film with epoxy resin

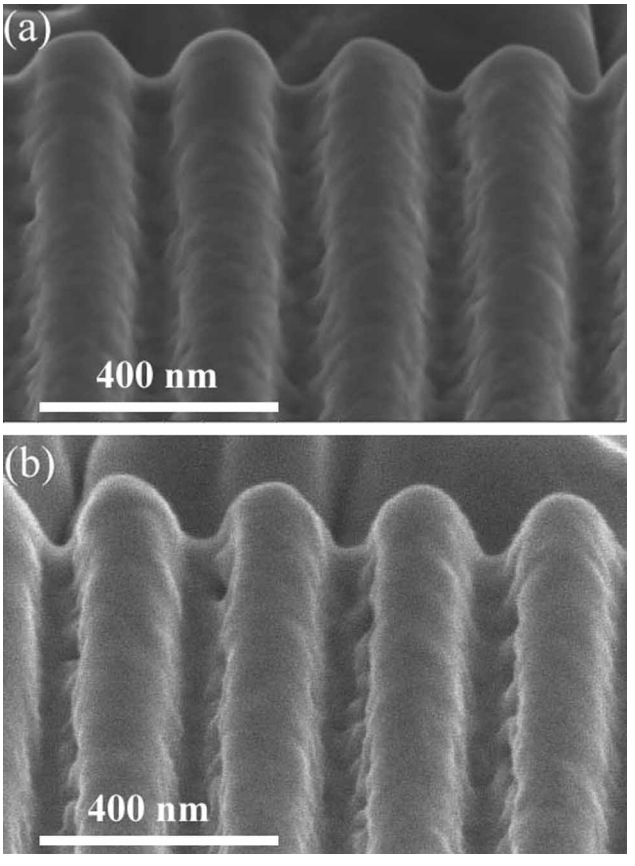

Figure 2. SEM images of silver gratings with the electron beam incident at 62° to the sample normal. The profile of these silver gratings can be described by a simple sinusoidal function with a pitch of 258 nm and a depth of 124 nm (*a*), 166 nm (*b*). The scale bar is 400 nm.

and dissolving the photoresist using acetone. This produces a smooth surface silver mono-grating with the same pitch and depth as the photoresist grating except with reversed profile. Figure 2 shows SEM images of silver gratings prepared using this technique. The gratings shown in figure 2 both have the same pitch of 258 nm but different depths of 124 nm (*a*) and 166 nm (*b*) respectively.

Figure 3 shows typical *p*-polarized wavelength-dependent reflectivity data which were obtained using a monochromator source in the range 400 nm to 850 nm for different incident angles at a fixed azimuthal angle $\phi = 0^\circ$ (the grating vector lying in the incident plane). Figure 3(*a*) shows reflectivity data for a grating with a ratio of depth to pitch of 0.48. Figure 3(*b*) shows the data for a deeper grating with a ratio of 0.58. Resonant modes are observed as minima in the wavelength-dependent reflectivity, which are circled in the figure. The SPP minima on these gratings are extremely broad and shallow since the modes are very much over-coupled. Previous modelling studies have shown far more pronounced minima, but these have been

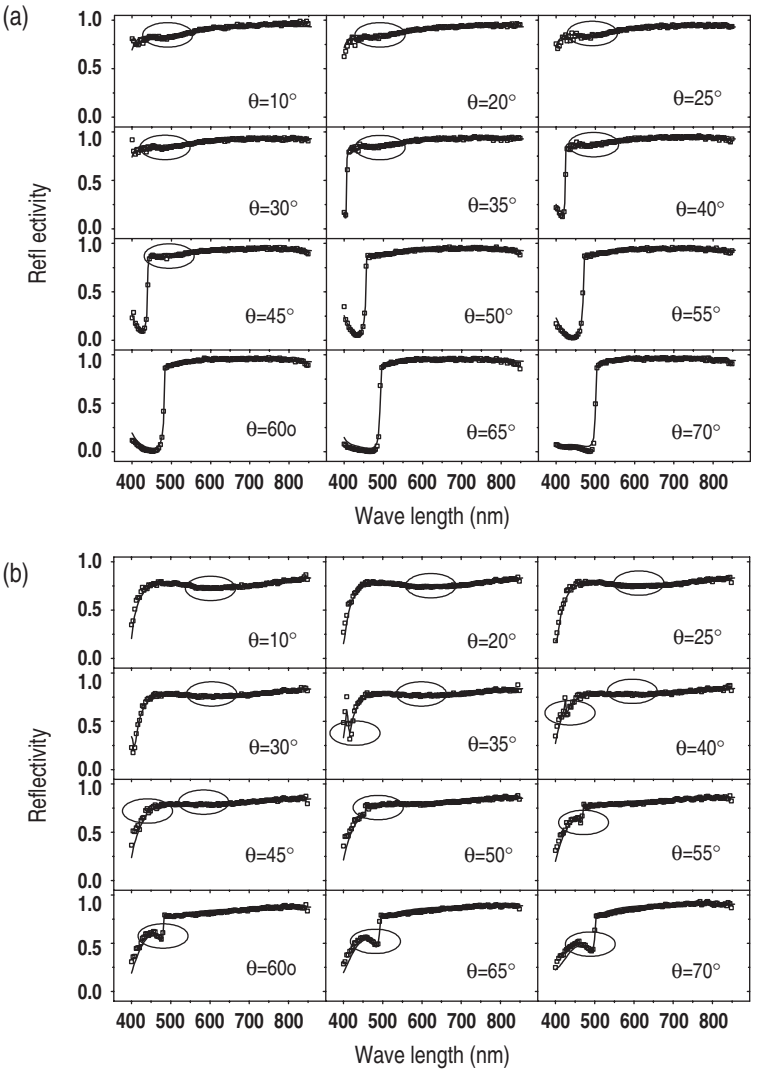

Figure 3. *p*-polarized experimental (circle) and modelled (solid line) wavelength-dependent reflectivity data obtained for different incident angles at a fixed azimuthal angle $\phi = 0^\circ$. (*a*) Grating with a depth of 124 nm. (*b*) Grating with a depth of 166 nm. The resonant minima are circled.

for narrow Gaussian grooved gratings, for which the coupling is much reduced. The gratings studied here are near-sinusoidal in character and thus the modes are over-coupled leading to the shallow modes.

The modelled response of the structure is obtained using the method reported elsewhere [11] and is based upon a non-orthogonal curvilinear coordinate transformation, which maps the grating profile onto a flat plane, as first proposed by Chandezon *et al*. [12]. Good agreement is obtained between the theoretical model

and the data, as shown by the full curves in figure 3. While fitting the reflectivity data, a simple sinusoidal function has been used to describe the gratings where the amplitude is largely determined from figure 2. Also the optical dielectric function of the silver used here ($\varepsilon_r = -409.58\,5 + 431.8 \times q - 199.9 \times q^2 + 49.33 \times q^3 - 6.385 \times q^4 + 0.342 \times q^5$ and $\varepsilon_i = 178.764 - 218.7 \times q + 105.2 \times q^2 - 24.60 \times q^3 + 2.772 \times q^4 - 0.119 \times q^5$, where $q = 10^{-15}\omega$ and ω is the angular frequency) is close to that reported by Nash *et al.* [13]. The small difference to that used by Nash *et al.* is caused by the roughness of the silver surface and the variable polycrystalline character of the silver film. For silver gratings with a pitch of 258 nm, the true zero-order spectrum region exists for wavelengths beyond 516 nm. In figure 3(*a*) with the 124 nm depth grating there is only one SPP minimum which occurs below 516 nm for all the different incident angles. Figure 3(*b*), with the 166 nm deep grating, shows that one SPP minimum has shifted above 516 nm, and is strongly radiative and very broad with a second SPP minimum appearing below 516 nm for some incident angles. Also from figure 3(*b*), we can see that these two minima shift in opposite directions as the incident angle increases. The minimum at the lower frequency has a blue shift and the minimum at the higher frequency has a red shift. Both modes tend towards the lightline/diffracted lightline at higher wavevectors. Hence the lower frequency mode tends towards the lightline, with a positive group velocity and a blue shift, whereas the higher frequency mode tends towards the diffracted lightline, with a negative group velocity and a red shift. However, from previous modelling studies [7] in which the dispersion curves of these standing wave SPP modes have been calculated it has been shown that the mode which experiences a red shift eventually passes through the diffracted lightline. There is some evidence of this in the data presented here, though it is by no means conclusive. In figure 3(*b*) at an angle $\theta = 70^\circ$, for example, at a wavelength slightly below the critical edge (around 500 nm) there is a clear minimum, which is not found in the data obtained from the shallower grating in figure 3(*a*).

The dispersion of the modes is shown in figure 4. The frequency of each resonant mode was obtained for 14 values of incident angles in the range 5° to 70°, and plotted against in-plane momentum k_x. Data indicated by squares are for the first-order SPP mode of the grating with a depth of 124 nm. Data given by triangles represent the first-order SPP mode of the grating with a depth of 166 nm. Data represented by circles are for the second-order SPP mode of the deeper grating. This has been shifted down enormously in frequency from originally being well into the diffracted region for a shallow grating to now being well inside the radiative region. (Also shown in the figure is a line describing the predicted dispersion of the second-order mode outside the first diffracted order light-line.) From comparison of these modes for different grating depth, we can see that for low aspect ratio gratings high-order modes only occur in the diffracted region, while for high aspect ratio gratings these modes may appear in the zero-order region as, with increasing depth, the SPP modes shift to lower frequency. We also notice from figure 4 that the flattest band occurs when its frequency approximates to that of a free photon having half the frequency of that which forms a zero momentum standing wave on the grating.

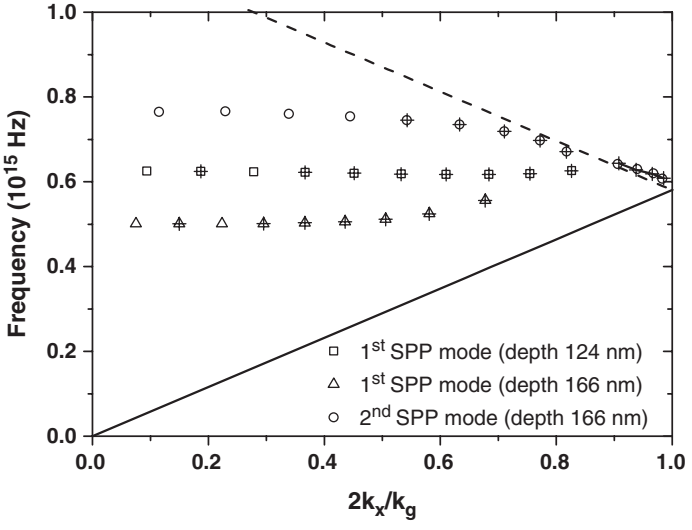

Figure 4. Dispersion curve of the SPP modes obtained from the reflectivity data for different incident angles. The solid line is the lightline, and the dashed line is the diffracted lightline. The open squares, circles and triangles are computed from the model used to produce the fits shown in figure 3. Squares are for the first-order SPP mode for the 124 nm deep sample; triangles are for the first-order SPP mode; and circles are for the second-order SPP mode for the 166 nm deep sample. The crosses and dots are the experimental data, the line indicates the mode just beyond the diffraction edge.

To understand the nature of these resonances it is instructive to investigate their optical field profiles. Figure 5 shows the $|H_z|$ (z is along the groove direction) component of the fields for 124 nm ($f = 0.625 \times 10^{15}$ Hz) and 166 nm ($f = 0.501 \times 10^{15}$ Hz, $f = 0.761 \times 10^{15}$ Hz) deep gratings at an incident angle $\theta = 5^{\circ}$. For the first-order resonance on the shallower 124 nm deep grating optical field maxima are observed on the tops of the gratings and also at the bottoms of the grating grooves. When the depth is increased to 166 nm the field maxima for the first-order resonance are still very similar to those of the shallower grating. However, for the second-order resonance, there are field maxima at the bottom of the grating grooves, a small maximum at the top of the grating grooves, and two extra field maxima found on the sides of the grating grooves. These additional maxima arise since the second-order mode has been scattered by twice the grating vector (as opposed to by a single grating vector, as for the first order mode), and thus its in-plane wavevector must be twice that of the first-order mode.

In summary reflectivity studies over the optical region, 400 to 850 nm, of deep silver monogratings with different depths are presented. Experimental data shows excellent agreement with the model predictions. From comparison of the modes for gratings with different depths, we verify the prediction that the SPP modes shift to lower frequency, and become flat-banded effectively localized modes with increasing grating depth.

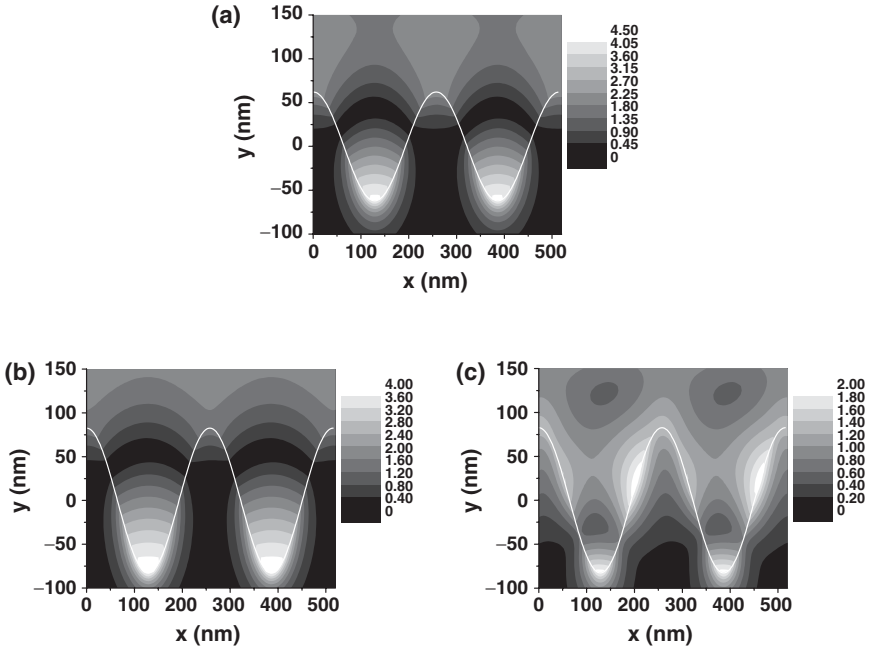

Figure 5. $|H_z|$ component of the fields for the SPP resonance for (*a*) $d = 124\,\text{nm}$, $f = 0.625 \times 10^{15}\,\text{Hz}$, $\theta = 5^\circ$, (*b*) $d = 166\,\text{nm}$, $f = 0.501 \times 10^{15}\,\text{Hz}$, $\theta = 5^\circ$, and (*c*) $d = 166\,\text{nm}$, $f = 0.761 \times 10^{15}\,\text{Hz}$, $\theta = 5^\circ$. The white line represents the grating profile.

Acknowledgments

Z. Chen acknowledges the financial support of an Overseas Research Studentship and from the University of Exeter.

References

[1] R.W. Wood, Proc. R. Soc. London A **18** 269 (1902).
[2] U. Fano, J. Opt. Soc. Am. **31** 213 (1941).
[3] A.A. Maradudin, in *Surface Polaritons*, edited by V.M. Agranovich and D.L. Mills (North-Holland, New York, 1982), p. 405.
[4] M.B. Sobnack, W.C. Tan, N. P. Wanstall, *et al.*, Phys. Rev. Lett. **80** 5667 (1998).
[5] J.A. Porto, F.J. Garcia-Vidal and J.B. Pendry, Phys. Rev. Lett. **83** 2845 (1999).
[6] W.C. Tan, T.W. Preist, J.R. Sambles and N.P. Wanstall, Phys. Rev. B **59** 12661 (1999).
[7] I.R. Hooper and J.R. Sambles, Phys. Rev. B **65** 165432 (2002).
[8] W.L. Barnes, T.W. Preist, S.C. Kitson and J.R. Sambles, Phys. Rev. B **54** 6227 (1996).
[9] W.L. Barnes, T.W. Preist, S.C. Kitson, *et al.*, Phys. Rev. B **51** 11164 (1995).
[10] H.E. Went and J.R. Sambles, Appl. Phys. Lett. **79** 575 (2001).
[11] N.P.K. Cotter, T.W. Preist and J.R. Sambles, J. Opt. Soc. Am. **12** 1097 (1995).
[12] J. Chandezon, M.T. Dupuis, G. Cornet and D. Maystre, J. Opt. Soc. Am. **72** 839 (1982).
[13] D.J. Nash and J.R. Sambles, J. Mod. Opt. **43** 81 (1996).